

Spectroscopic Investigation on the Origin of Photoinduced Carrier Generation in Semiconducting InGaO and InGaZnO Films

Deok-Yong Cho,[†] Jeong Hwan Kim,[‡] Un Ki Kim,[‡] Yoon Jang Chung,[‡] Jaewon Song,[‡]
Cheol Seong Hwang,^{*,‡} Jae-Min Lee,[†] and Se-Jung Oh^{*,†}

CSCMR & FPRD, Department of Physics and Astronomy, Seoul National University, Seoul 151-747, Korea,
and WCU Hybrid Materials Program, Department of Materials Science and Engineering and Inter-university
Semiconductor Research Center, Seoul National University, Seoul 151-744, Korea

Received: April 28, 2010

We investigated the electronic structures of defective semiconducting InGaO and InGaZnO films using X-ray photoelectron spectroscopy. The defects were created intentionally using an intensive Ar-ion bombardment on the films. After Ar bombardment, a subgap state emerged above the valence band edge, which decreased the band gap to <2 eV, suggesting the possibility of electron–hole pair creation even under visible light illumination. Also, the defect states were found to have metal sp characters, being related to oxygen deficiencies in the n-type semiconducting oxides. Therefore, eliminating the oxygen deficiency in the semiconducting oxide films is essential for preventing the photoinduced degradation in thin-film field effect transistors.

1. Introduction

Photoinduced carrier generation in semiconducting oxide (SO) thin films has attracted increasing attention because it significantly degrades the stability of thin-film field effect transistors (TFTs) under bias and temperature stress conditions.^{1–3} The photoinduced degradation of TFTs under extreme ultraviolet (UV) illumination ($\lambda < 350$ nm) can be understood easily because electron–hole pairs that overcome the band gap (typically ~ 3 to 3.5 eV) might be created by the photoexcitation, and one type of the carrier is trapped in the gate insulator (GI) or at the GI–semiconductor interface under high gate bias application. However, the degradation occurs even under the visible light illumination,^{4,5} which cannot be explained by direct excitation from the valence band (VB) to the conduction band (CB) because the photon energy is much lower than the band gap. Thus, the visible-light-induced degradation should occur through the introduction of additional gap states that can produce an electron–hole pair under visible light illumination.

It was reported that such a gap state (GS) was induced by a H₂O diffusion with bias temperature instability (BTI) under the visible light illumination.⁶ However, the diffusions of exterior molecules or radicals seem not to be a necessary condition; it was also reported that the BTI under the illumination occurred even without any environmental influence, which could be prevented by an efficient passivation layer.⁷ This suggests that there are some inherent reasons that may cause a GS. In the SO materials, such as the In–Ga–Zn–O system, the defect-induced GSs are frequently related to oxygen deficiencies (oxygen vacancies or metal ion interstitials). However, it is not clear how the oxygen deficiency causes a GS that is deep enough to induce the visible light photoexcitation with reducing the band gap to <2 eV because defect states related to the oxygen deficiency tend to induce rather shallow trap levels only near

the conduction band edge.³ Therefore, it is meaningful to analyze the GS in the damaged SO by spectroscopic methods.

However, the defect density of well-prepared SO materials for reasonable TFT operations is too low to be analyzed by general spectroscopic techniques. Therefore, a high density of defects in SO films was formed by the excessive Ar-ion bombardment in order to study the influence of the defects. The significance of the Ar-ion bombardment effects on the physical and chemical properties of samples depends on the kinetic energy (or acceleration voltage) of the Ar plasma.⁸ The Ar-ion bombardment with a moderate acceleration voltage (<1 keV) only removes adsorbates, such as hydrocarbons, without degrading the stoichiometry of the sample, whereas bombardment with a high acceleration voltage (>1 keV) damages the sample intensively, altering the structure and compositions.

2. Experimental Methods

This article reports the evolution of the VB spectra of the representative SO, InGaO and InGaZnO films, upon Ar-ion bombardment with 2 keV acceleration using X-ray photoelectron spectroscopy (XPS). The 50 nm thick InGaO and InGaZnO films were deposited on Si(100) substrates at room temperature by rf magnetron sputtering using polycrystalline ceramic targets. The binding energies (BE) and XPS peak intensities of the In 3d, Ga 2p, and Zn 2p core levels showed that the cations in both films have nominal valences of In³⁺, Ga³⁺, and Zn²⁺, and the empirical formulas should be InGaO₃ and In₂Ga₂ZnO₇ for the respective films.⁹ Intentional Ar ion bombardment was performed in an Ar environment (5×10^{-8} Torr) with an acceleration voltage of 2 keV for 10 s. The film was etched to within 1 nm. XPS was performed with a monochromated Al K α source ($h\nu = 1486.6$ eV) and synchrotron radiation ($h\nu = 700, 130, \text{ and } 90$ eV) at the 8A2 beamline in the Pohang Light Source (PLS).

3. Results and Discussion

Figure 1 shows the VB XPS spectra of the (a) InGaO and (b) InGaZnO films before and after Ar-ion bombardment. The

* To whom correspondence should be addressed. E-mail: cheolsh@snu.ac.kr (C.S.H.), sjoh@snu.ac.kr (S.-J.O.). Tel: +82-2-880-7535 (C.S.H.), +82-2-880-6609 (S.-J.O.).

[†] CSCMR & FPRD, Department of Physics and Astronomy.

[‡] WCU Hybrid Materials Program, Department of Materials Science and Engineering and Inter-university Semiconductor Research Center.

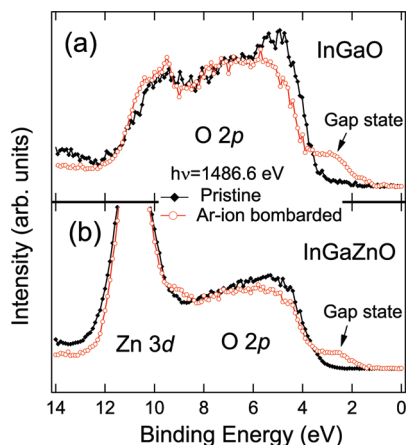


Figure 1. VB XPS spectra of the (a) InGaO and (b) InGaZnO films before and after Ar-ion bombardment taken at $h\nu = 1486.6$ eV. A gap state (GS) emerged after the Ar-ion bombardment.

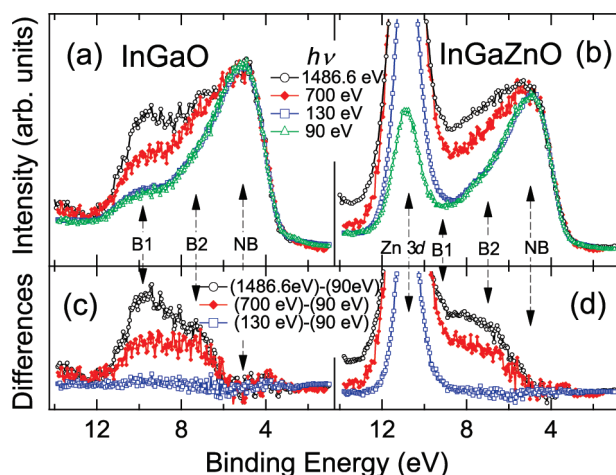


Figure 2. VB XPS spectra of pristine (a) InGaO and (b) InGaZnO films taken with $h\nu = 1486.6, 700, 130,$ and 90 eV and their difference spectra (c, d) from those of $h\nu = 90$ eV. B1(B2) corresponds to the metal $s(p)$ -O 2p hybridized state, and NB denotes the nonbonding O 2p states.

VB of InGaO comprises mainly the O 2p state only, whereas the VB of InGaZnO consists mainly of O 2p and Zn 3d states. The VB edge energies of the pristine films, which were estimated by extrapolating the lowest BE feature, were approximately 3 eV. Because the band gaps of the two SO films are approximately 3.4 eV,¹⁰ the CB edge energies are very close to the Fermi level (E_F), indicating the n-type nature of these films. The spectra of the Ar-ion bombarded films were shifted to a lower binding energy (BE) by ~ 0.5 eV in order to match the overall VB features with those of the pristine films. The BE difference from that of the pristine films originates partly from the overall higher BE shift due to the E_F increase and partly from the space charging effect in the poorly conducting samples. A gap state (GS) was clearly observed above the VB edge in both spectra of the InGaO and InGaZnO films. The GSs increased the VB edge energy of the SO films by >1 eV and decreased the band gap to <2 eV, suggesting a significant increase in the visible light photoexcitation from the GS in the Ar-ion bombarded samples.

XPS of the pristine SO films was performed at various photon energies to obtain detailed information on the orbital characteristics and density of states (DOS). Figure 2 shows the VB XPS spectra of pristine (a) InGaO and (b) InGaZnO films taken with $h\nu = 1486.6, 700, 130,$ and 90 eV and their difference

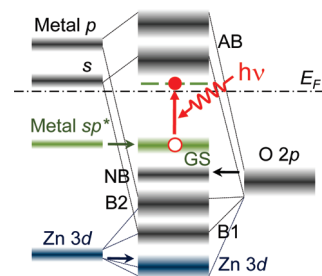


Figure 3. Schematic diagram of the energy levels resulting from metal sp -O 2p hybridization. In the case of InGaZnO, the Zn 3d levels participate in hybridization. Ar-ion bombardment forms the gap states (GS) above the VB as well as the shallow defect states beneath the CB (short bars) so that the electron-hole pairs would be created even with visible light illumination.

spectra [(c) and (d)] from those of $h\nu = 90$ eV. The VB spectra were normalized to the intensity of the nonbonding O 2p features near BE ~ 5 eV. The overall features in the VB spectra appear to evolve with increasing photon energy. Generally, the $h\nu$ dependence in the soft X-ray photoemission spectra originates from two factors: the subshell photoionization cross section and electron inelastic mean free path (IMFP). Because the IMFP varies slowly with the kinetic energy of the photoelectron, it cannot explain the abrupt spectral evolution in the VB energy range. Instead, the photoionization cross section varies abruptly with the incident photon energy depending on the orbital states. Therefore, the difference spectra (Figure 2c,d) can be used to analyze the orbital states in the VB.

In the case of InGaO, the two features denoted by “B1” and “B2” were enhanced as the photon energy increased in comparison with the feature denoted as “NB” in Figure 2a,c. All three features must be from the O 2p states, whereas the different $h\nu$ dependence further reflects the different degree of hybridization between the O 2p states and metal sp states. If it were not for the orbital hybridization, the metal sp states (In 5s, Ga 4s) would be completely unoccupied and the O 2p states would be completely filled. The metal s states have ~ 3 eV lower energy than the metal p states.¹¹ The metal sp -O 2p hybridization overlaps the orbital wave functions, resulting in parts of the metal sp states being filled, forming bonding states with the O 2p states that have energies lower than the nonbonding O 2p states. Therefore, the B1(B2) state should be attributed to the metal $s(p)$ -O 2p bonding states, and the NB state is due to the nonbonding O 2p states.¹²

In the case of InGaZnO, the hybridized orbital states were similar to the case of InGaO except for the inclusion of a shallow Zn 3d core level, as shown in Figure 2b,d. Therefore, the overall VB features were similar to the case of InGaO except for the slight energy differences due to Zn 3d hybridization. The Zn 3d level at BE ~ 10.8 eV also hybridizes with the O 2p states and, consequently, the metal sp states. This complex hybridization raises the energies of the B1 and B2 states slightly.¹² The B2 feature in Figure 2c is extinguished below the onset BE at ~ 6 eV, whereas that in Figure 2d is extinguished below a lower onset BE (<5 eV). This highlights the role of the Zn 3d levels.

The GS cannot be attributed to the O 2p state because any hybridized state should have lower energy than that of the NB O 2p state (see Figure 3). Therefore, the GS should have metal orbital characteristics. The partial electron occupation in the GS originates from defects in the damaged SO films. The defect states might be related to oxygen deficiencies, such as the oxygen vacancies or metal ion interstitials. The intensity of the NB state near BE ~ 5 eV decreased after Ar-ion bombardment,

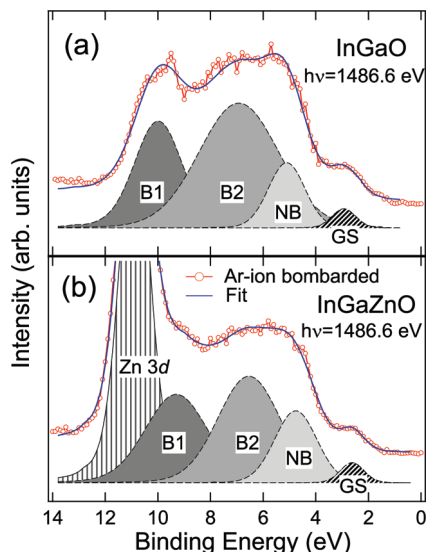


Figure 4. VB XPS spectra of the Ar-ion bombarded (a) InGaO and (b) InGaZnO films with their fitting lines. Each contribution is shown separately.

which is in contrast to the case of the bonding states (Figure 1). This suggests a decrease in the total number of oxygen atoms because the number of the NB O 2p states might decrease with a decreasing number of oxygen atoms, whereas the hybridized states could survive by charge compensation from the metal sites; an oxygen deficiency will donate electrons back to the metal sites, even though the amount of the back-donation can vary depending on the detailed balance in the SO films. Therefore, the oxygen deficiency should be responsible for the partial occupation of the metal sp electrons in the GS above the VB edge.

Figure 3 summarizes the orbital configuration. The possible electron–hole pair formation under the visible light illumination is also indicated. In the pristine SO films, hybridization of the O 2p orbitals with the metal s and p orbitals splits the O 2p band into B1, B2, and NB states by lowering the corresponding B1 and B2 states below the E_F (in the VB) and raising the corresponding antibonding states (AB) above the E_F (in the CB).¹³ Zn 3d hybridization changes the energies of the O 2p B1/B2 states slightly. Finally, in the presence of defects, as in the Ar-ion bombarded samples, a GS is formed above the pristine VB edge.

Figure 4 shows the VB spectra with the fitting lines along with their decomposed features ((Zn 3d), B1, B2, NB, and the GS). The DOS of the GS can be approximated using the intensity ratio of each feature with the averaged photoionization cross sections for metal s and p states and the O 2p state.¹⁴ Assuming that the GS has mixed metal s orbital character only, the number of the GS was determined to be ~ 0.05 states per oxygen atom. This value corresponds to the DOS of $\sim 10^{21} \text{ cm}^{-3}$ for both InGaO and InGaZnO films, which is in the same order of magnitude as the as-grown low-quality sample in a previous report.¹⁵ The decreased intensity of the GS and improved TFT characteristics upon thermal annealing also suggests that the GS plays a major role in the photoinduced carrier generation.¹⁶ Without photoillumination, this deep level barely contributes to conduction because the band-gap energy is still much higher than the thermal fluctuation energy. However, this GS enables

the production of an electron–hole pair by visible light illumination through photoexcitation. In n-type SO materials, the defect states relevant to an oxygen deficiency form shallow defect states beneath the CB edge.¹⁷ Photoexcitation from the VB GS to those shallow defect states (denoted as short bars above the E_F in Figure 3) can generate bound or free carriers, as depicted in Figure 3. Therefore, it is essential to eliminate the defects in SO films to improve the TFT stability.

4. Conclusion

In conclusion, a metal sp GS emerged above the VB edge in Ar-ion bombarded InGaO and InGaZnO films. Combined with the shallow defect states near the CB edge, this can act as a center for photoinduced electron–hole generation in damaged TFTs. Although the GS observed in this XPS study was certainly an exaggeration by intentional Ar-sputter etching, these results may provide a crucial clue to understanding the photoinduced BTI characteristics of TFTs. Oxygen deficiency in these SO films generated the GS near the VB edge as well as the electron trap sites below the CB edge. It is clear that this process is detrimental to the stability of the performance of TFTs even with a very low density, although further studies on the trapping “ability” (or the localization of the defect states) of the GS are required to clarify this issue.

Acknowledgment. This study was supported by the NRF, funded by the Ministry of Education, Science and Technology (MEST), through the Converging Research Center Program (2009-0081961), WCU Program (R31-2008-000-10075-0) and Acceleration Research Program (R17-2008-033-01000-0), and by Samsung Advanced Institute of Technology. Experiments at PLS were supported, in part, by MEST and POSTECH.

References and Notes

- (1) Takechi, K.; Nakata, M.; Eguchi, T.; Yamaguchi, H.; Kaneko, S. *Jpn. J. Appl. Phys.* **2009**, *48*, 010203.
- (2) Fung, T.-C.; Chuang, C.-S.; Nomura, K.; Shieh, H.-P. D.; Hosono, H.; Kanicki, J. *J. Disp. Technol.* **2008**, *9*, 21.
- (3) Kamiya, T.; Nomura, K.; Hosono, H. *J. Disp. Technol.* **2009**, *5*, 273.
- (4) Barquinha, P.; Pimentel, A.; Marques, A.; Pereira, L.; Martins, R.; Fortunato, E. *J. Non-Cryst. Solids* **2006**, *352*, 1756.
- (5) Görrn, P.; Lehnhardt, M.; Riedl, T.; Kowalsky, W. *Appl. Phys. Lett.* **2007**, *91*, 193504.
- (6) Lee, K.-H.; Jung, J. S.; Son, K. S.; Park, J. S.; Kim, T. S.; Choi, R.; Jeong, J. K.; Kwon, J.-Y.; Koo, B.; Lee, S. *Appl. Phys. Lett.* **2009**, *95*, 232106.
- (7) Park, S.-H. K.; Hwang, C.-S.; Ryu, M.; Yang, S.; Byun, C.; Shin, J.; Lee, J.-I.; Lee, K.; Oh, M. S.; Im, S. *Adv. Mater.* **2009**, *21*, 678.
- (8) Taguchi, M.; Hamaguchi, S. *J. Appl. Phys.* **2006**, *100*, 123305.
- (9) Cho, D.-Y.; Song, J.; Hwang, C. S. *J. Phys. Chem. C* **2009**, *113*, 20463.
- (10) Nomura, K.; Ohta, H.; Takagi, A.; Kamiya, T.; Hirano, M.; Hosono, H. *Nature* **2004**, *432*, 488.
- (11) Cho, D.-Y.; Song, J.; Hwang, C. S.; Choi, W. S.; Noh, T. W.; Kim, J.-Y.; Lee, H.-G.; Park, B.-G.; Cho, S.-Y.; Oh, S.-J.; Jeong, J. H.; Jeong, J. K.; Mo, Y.-G. *Thin Solid Films* **2009**, *518*, 1079.
- (12) Wei, S.-H.; Zunger, A. *Phys. Rev. B* **1988**, *37*, 8958.
- (13) Cho, D.-Y.; Song, J.; Na, K. D.; Hwang, C. S.; Jeong, J. H.; Jeong, J. K.; Mo, Y.-G. *Appl. Phys. Lett.* **2009**, *94*, 112112.
- (14) Yeh, J. J.; Lindau, I. *At. Data Nucl. Data Tables* **1985**, *32*, 1.
- (15) Nomura, K.; Kamiya, T.; Yanagi, H.; Ikenaga, E.; Yang, K.; Kobayashi, K.; Hirano, M.; Hosono, H. *Appl. Phys. Lett.* **2008**, *92*, 202117.
- (16) Nomura, K.; Kamiya, T.; Hirano, M.; Hosono, H. *Appl. Phys. Lett.* **2009**, *95*, 013502.
- (17) Kamiya, T.; Hosono, H. *NPG Asia Mater.* **2010**, *2*, 15.